# Inverse Leidenfrost effect: drops gliding on a bath

# Supplementary Materials

The supplementary materials contain:

- Supplementary Figures 1,2 and 3
- Supplementary table 1, with values of the physical parameters used in models and simulation
- Description of supplementary movies
- Detailed theoretical models: for the thickness of the vapor film in cold Leidenfrost situation and full calculation (in a simplified geometry) of the propelling and friction forces.

## I. SUPPLEMENTARY FIGURES

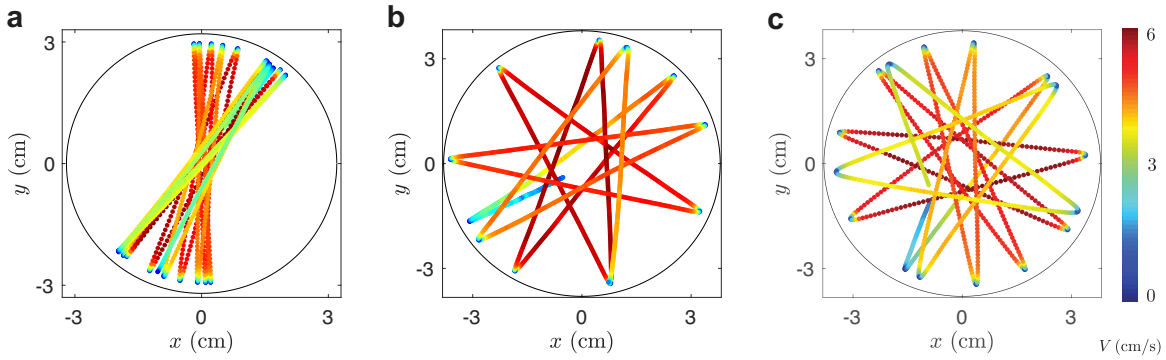


Figure 1: Examples of drop trajectories. All drops are ethanol, with radius $R = 1.4$ mm. The color code (on the right) indicates the drop velocity, from $V = 0$ cm/s (dark blue) to $V = 6$ cm/s (dark red). Depending on the initial conditions, the drop trajectory forms stars with different number of branches.



www.pnas.org/cgi/doi/10.1073/pnas.1812288115

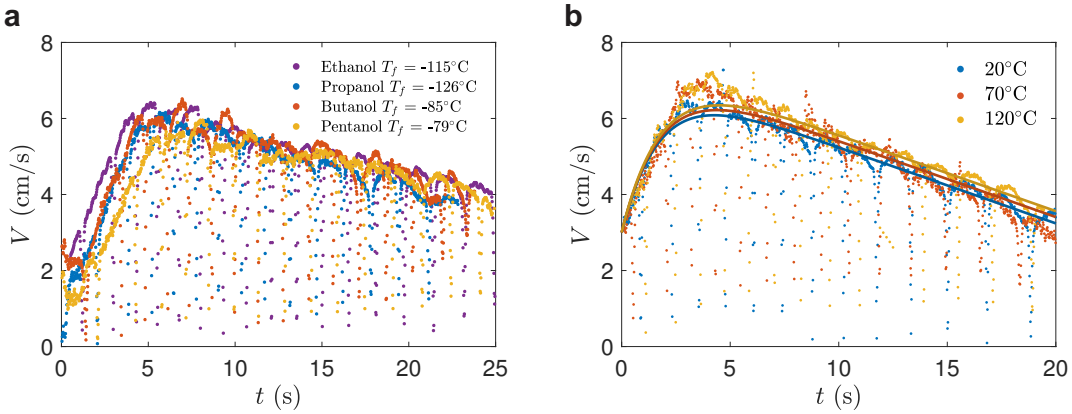


Figure 2: **Thermal effects on velocity profiles a.** Comparison of the velocity profiles $V(t)$ of 5 alcohol drops with similar initial velocities. The drops have similar radius $R = 1.4$ mm and heat capacity $\frac{4}{3}\pi\rho R^3 c_p$, but different freezing temperatures, from $T_f$ = -126°C for propanol to $T_f$ = -79°C for pentanol. **b.** Velocity profiles $V(t)$ of silicon oil drops with varying initial temperatures.

Table I: Values of physical parameters used in the model and simulation

| **Quantity** | **Symbol** | **Value** |
|---|---|---|
| Liquid nitrogen | | |
| surface tension of liquid nitrogen | $\gamma_N$ | 8.85 mN/m |
| density of liquid nitrogen | $\rho_N$ | 808 kg/m$^3$ |
| latent heat of vaporization | $L_v$ | 2 x 10$^5$ J/kg |
| density of nitrogen vapor | $\rho_v$ | 1.7 kg/m$^3$ |
| viscosity of nitrogen vapor | $\eta_v$ | 12.9 $\mu$Pa.s |
| thermal conductivity of nitrogen vapor | $\lambda$ | 18.7 mW/m/K |
| Silicone oil | | |
| density | $\rho$ | 930 kg/m$^3$ |
| specific heat | $c_p$ | 1600 J/kg/K |
| Ethanol | | |
| density at -115° C | $\rho$ | 900 kg/m$^3$ |
| specific heat | $c_p$ | 2400 J/kg/K |

## II. SUPPLEMENTARY MOVIES

**Movie S1** Top view of an ethanol drop with radius $R = 1.4$ mm seeded with dark particles, just after being deposited on a liquid nitrogen bath. Slowed down 1.5 times.

**Movie S2** Top view of a polyethylene particle (with radius $R = 1.0$ mm and density $\rho = 900$ kg/m$^3$) sitting on a liquid nitrogen bath. The particle is marked with black dots to visualize potential rotations. The velocity $V$ of the particle is plotted as a function of time in the figure below. Similarly to drops, the particle is accelerated and glides in straight lines across the bath.

**Movie S3** Position and velocity $V(t)$ of a silicone oil drop (with radius $R = 1.4$ mm) while gliding on a liquid nitrogen bath. The drop crosses the bath in straight lines. Its dynamics can be decomposed in 3 phases: (1) acceleration, in the first 5 seconds (2) constant deceleration, that lasts 25 seconds and (3) a constant velocity phase, that lasts for the whole drop lifetime. The movie is shown in real time.

**Movie S4** Top view of a silicone oil drop (with radius $R = 1.4$ mm) while gliding on a liquid nitrogen bath. In the end of the movie, the cold drop encounters an ice cristal and sinks. The amount of vapor generated is small, indicating that the drop temperature is close to that of the bath. The movie is in real time.

**Movie S5** Movie extracted from simulations, showing the dynamic mesh of the ALE-FEM simulation with the pseudo-elastic node movement and the mesh reconstruction whenever the deformation of the elements gets to intense.

**Movie S6** Simulation of inverse Leidenfrost levitation of a drop with radius $R = 1.0$ mm and viscosity $\eta = 16$ mPa.s.

**Movie S7** Top view of a liquid nitrogen drop (with radius $R = 1.8$ mm levitating above a liquid nitrogen bath, more than 10 minutes after being deposited. The drop adopts a circular trajectory and keeps a constant velocity $V^* \simeq 2.2 \pm 0.2$ cm/s while rotating. The movie accelerated two times.

**Movie S8** Top view of a liquid nitrogen drop (with initial radius $R = 1.1$ mm) deposited on an ethanol bath. Due to the difference of temperature between the drop and the bath, the nitrogen drop evaporates and remains in levitation above the bath. Similarly to what is seen in the inverse Leidenfrost situation, it is self-propelled and crosses the bath in straight lines. Its velocity $V$ is plotted as a function of time $t$. The movie is in real time.

## III. NUMERICAL METHOD

The numerical simulation is based on a finite element method of the incompressible 2d Cartesian Navier-Stokes equations with sharp interfaces that are aligned with the mesh, which is an ideal approach to capture the thin gas layer between the droplet and the bath. To account for the motion of the droplet and the bath interface, the mesh nodes are co-moved with the interfaces combined with an arbitrary Lagrangian-Eulerian method. All nodal positions in the bulk are updated by treating the mesh as a pseudo-elastic solid which is deformed by the movement of the interfaces. The dynamics of the interfaces is governed by the conventional kinematic and dynamic boundary conditions. Since the shifting of the nodes eventually causes large mesh distortions, we reconstruct the mesh whenever the quality falls below a specific threshold. During this remeshing, the interfaces are captured by splines to generate a new mesh and the previous nodal data are interpolated to the new mesh (see Supplementary Movie 5).

It is always ensured that the element size in the thin gas layer is very fine whereas it gets coarser in the far field. To solve the flow, conventional triangular Taylor-Hood elements are used. At the interfaces, the Laplace pressure causes a discontinuity of the pressure whereas evaporation causes a jump in the normal velocity component due to the density ratio. To that end, nodes on the interface store two pairs of velocity and pressure data, i.e. for both sides of the interface, which are coupled across the interface via Lagrange multipliers. The two-dimensional simulation domain has a size of 77 mm in width and 45 mm in height. The bath-gas interface is placed at a height of 20 mm from the bottom with a contact angle of 20° with respect to the side wall. No-slip boundary conditions are imposed on all exterior boundaries, except for the upper boundary, where a traction-free outlet is used. The implementation has been done using the framework OOMPH-LIB.

## IV. THEORETICAL MODELS

### A. Thickness of the vapor film in cold Leidenfrost situation

#### 1. *Drop-induced evaporation*

Here we describe the calculation done to determine the thickness of the vapor film $h$ sustaining a hot drop deposited on a cryogenic bath (in an inverse Leidenfrost situation), as is used in the paper. In this calculation, the consequences of phase change (namely freezing of the drop) is neglected: we consider that it happens instantly, and that the specific heat of the frozen drop is the same as the specific heat of the liquid drop. A more detailed model (taking into account thermal effects during the phase change) can be found in the paper of M. Adda-Bedia *et al.* (Langmuir, 2016). The results they obtain are very close to the ones presented here, with a cooling down time a bit longer due to the addition of a freezing time.

We seek here for a expression of $h$ and its dependency with time. This is done by combining 3 elements: vapor generation, pressure buildup within the confined vapor, and the cooling dynamics of the drop.

**(1) Vapor generation.** In this inverse Leidenfrost effect, heat from the (hot) drop diffuses across the film and locally vaporises the (cryogenic) bath. The vapor flux $q$ generated by the pool is determined by the rate at which heat diffuses through the film. In scaling laws, this can be written $\lambda\frac{\Delta T}{h}R^2$ with $\lambda$ the conductivity of vapor, $\Delta T/h$ the gradient of temperature through the film (with thickness $h$), and $R^2$ the surface of contact between the drop and the bath. Energy transfer from the drop generates evaporation of the bath, where the rate of energy dissipated in the bath is $L_v\frac{dM}{dt}$ with $M$ the mass of vapor generated per second under the drop and $L_v$ the latent heat of vaporisation of liquid nitrogen. Equalizing these two expressions gives a first equation $\lambda\frac{\Delta T}{h}R^2 \sim L_v\frac{dM}{dt}$, from which the vapor flux $q$ can be determined. Indeed, we also have $\rho_v q \sim \frac{dM}{dt}$, denoting $\rho_v$ the vapor flux, so that:

$$q \sim \frac{\lambda}{\rho_v L_v}\frac{\Delta T}{h}R^2 \tag{1}$$

**(2) Pressure buildup within the film.** The escaping vapor is confined into the film, which creates an overpressure that sustains the drop. The overpressure $\Delta p$ within the film is calculated using lubrication theory, which, in scaling laws is written: $\frac{\Delta p}{R} \sim \eta_v\frac{u}{h^2}$. $\Delta p/R$

is the pressure gradient (along the drop with radius $R$), $u$ the characteristic velocity of the vapor within the film, and $h$ the film thickness. Mass conservation within the film also gives $q \sim Rhu$. By combining lubrication, mass conservation and thermodynamics (equation 1), we finally find $h$ for any given temperature difference $\Delta T$ between the drop and the bath:

$$h \sim \left( \frac{\eta_v \lambda \Delta T R}{\rho g \rho_v L_v} \right)^{1/4} \tag{2}$$

By denoting $\Delta T_0$ the initial difference of temperature (at a time $t = 0$), and $h_0$ the corresponding initial film thickness the previous expression can be re-written:

$$h \sim h_0 \left( \frac{\Delta T}{\Delta T_0} \right)^{1/4} \text{ with } h_0 \sim \left( \frac{\eta_v \lambda \Delta T_0 R}{\rho g \rho_v L_v} \right)^{1/4} \tag{3}$$

**(3) Drop cooling.** The variation of $h$ with time can be finally deduced from the cooling dynamics of the drop, which acts as a finite reservoir of (thermal) energy. Then, the rate at which the internal energy of the drop decreases must equal the rate at which energy diffuses across the vapor film (which is $\sim \lambda \frac{\Delta T}{h} R^2$). Denoting $c_p$ the specific heat of the drop, the drop internal energy is $\rho R^3 c_p \Delta T$; and energy balance is written $\rho R^3 c_p \frac{d}{dt} \Delta T \sim -\lambda \frac{\Delta T}{h} R^2$. Using the previous expression for $h$ (eq. 3) the differential equation becomes $\frac{d\Delta T}{\Delta T^{3/4}} = -t/(\rho R c_p h_0/\lambda)$. Integration then gives:

$$\Delta T = \Delta T_0 (1 - t/\tau)^4, \text{ with } \tau \sim \frac{4 \rho R c_p h_0}{\lambda} \tag{4}$$

$\tau$ corresponds to the time it takes for the drop to cool down, from ambient temperature to the liquid nitrogen temperature: for millimeter-sized drops, this time is of the order of 20 s. Inserted in equation 3, equation 4 it finally gives:

$$h \sim h_0 \, (1 - t/\tau) \tag{5}$$

a linear decrease of $h$ that indeed fits nicely the drop dynamics.

*2. Film thickness in presence of both residual bath evaporation and drop-induced evaporation*

To completely model the film thickness, one needs to take into account the constant bath evaporation (independent of the drop presence). The total vapor flow below the drop is the

sum of two vapor fluxes, namely $q_1$ (drop-induced) and $q_2$ (from the residual evaporation of the bath, due to radiative heat transfert). From equation 1, we have:

$$q_1 \sim \frac{\lambda}{\rho_v L_v} \frac{\Delta T}{h} R^2, \tag{6}$$

and the vapor flux generated by radiative heat transfert can then be written as

$$q_2 \sim \frac{\sigma \left(T_{amb}^4 - T_N^4\right) R^2}{\rho_v L_v}. \tag{7}$$

Here, we denote $\sigma$ the Stefan-Boltzmann constant, $T_{amb}$ and $T_N$ the ambient and liquid nitrogen temperatures respectively. By noting $q = q_1 + q_2$ the total vapor flux under the drop, the film thickness $h(t)$ is then deduced by combining (as before) mass conservation and a vertical balance of forces. Mass conservation implies that $q = q_1 + q_2 = Rhu$. Lubrication equations applied to the vapor film impose that $\frac{\Delta p}{R} \sim \eta_v \frac{u}{h^2}$. Finally, the overpressure $\Delta p$ compensates the weight of the drop (enabling levitation) which is written $\Delta p \sim \rho g R$. By combining these equations, we find that:

$$h^3 \sim (q_1 + q_2) \frac{\eta_v}{\rho g R}. \tag{8}$$

using equations 6 and 7, $h$ can be written as:

$$h(t)^4 \sim \frac{\eta_v \lambda R \Delta T}{\rho g \rho_v L_v} + \frac{\eta_v R \sigma \left(T_{amb}^4 - T_N^4\right)}{\rho g \rho_v L_v} h(t) \tag{9}$$

By introducing the expressions of the initial Leidenfrost film thickness $h_0$ (from equation 3) and the film thickness generated by the bath residual evaporation $h_{N_2} \sim \left(\frac{\eta_v \sigma (T_{amb}^4 - T_N^4) R}{\rho_v \rho g L_v}\right)^{1/3}$ (as obtained in equation 7 in the manuscript), the previous expression can be simplified:

$$h(t)^4 \sim h_0^4 \left(\frac{\Delta T(t)}{\Delta T_0}\right) + h_{N_2}^3 h(t) \tag{10}$$

The drop cooling dynamics (see previous paragraph) finally impose a second relation between $h$ and $\Delta T$:

$$\rho R^3 c_p \frac{d}{dt} \Delta T \sim -\lambda \frac{\Delta T}{h} R^2. \tag{11}$$

Solving both equations 10 and 11 finally gives access to the variations of the film thickness $h(t)$. This system of equations can be simplified by solving them separately: indeed, during the first ten seconds of the drop lifetime, the relatively hot drop makes the bath evaporate rapidly. When calculating the two vapor fluxes for a millimeter-sized drop just deposited on the bath, we obtain from equations 6 and 7 that initially $q_2 \simeq q_1/100$. This implies that the residual evaporation of the bath can be neglected when considering the drop cooling dynamics (which happens mostly during the first ten seconds). Concretely, this means that equation 11 can be simplified by replacing $h$ with $h_0$.

By solving equation 11 with $h \simeq h_0$ and replacing the solution $\Delta T(t)$ in equation 10, we finally obtain a simple solution for $h_{tot}$, as the unique real and positive root of the following fourth-order polynomial equation:

$$h(t)^4 \sim h_0^4 \left(1 - t/\tau\right)^4 + h_{N_2}^3 h(t) \tag{12}$$

### B. Propelling and friction forces in a simplified floating disk model

Here, we propose to model the forces (propulsion and friction) applying on a levitating drop a simplified geometry. We consider a simple case where the film thickness difference $\Delta h$ is imposed. Following Dupeux *et al.*, we model the asymmetric film generated below a solid cylindrical object, and, similarly to what is done for spherical droplets, we denote $\Delta h$ the asymmetry between the two sides of the film (see figure 3). The radius of the cylinder is $R$ and its thickness $e$. The film thickness $h$ varies here between $h_0 + \Delta h$ in $x =$ - $2R$ to $h_0$ in $x = 0$, where is $x$ chosen as the direction in which the disk is tilted. Finally, $V$ is the disk velocity in the $x$ direction.

Similarly to Leidenfrost drops, we consider that the disk floats above the surface thanks to a continuous vapor flow arising from the evaporation of the surface with a characteristic velocity $j$. The thermal gradient through the film fixes $j$, though an energy balance:

$$\rho_v L_v j = \frac{\lambda \Delta T}{h} \tag{13}$$

with $\rho_v$ the vapor density, $L_v$ the latent heat of vaporization of the substrate and $\lambda$ the vapor conductivity.

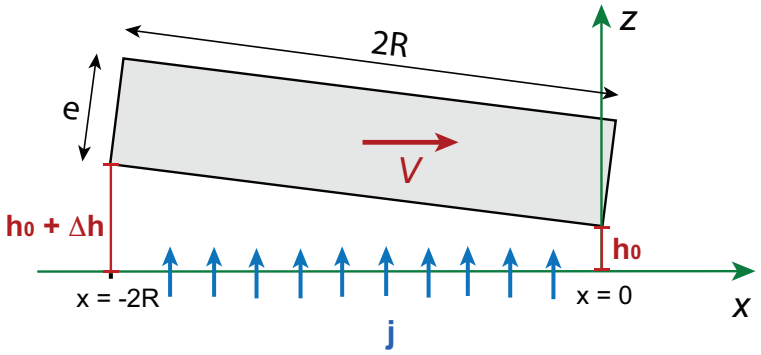


Figure 3: Floating disk model. The disk has a radius $R$ and a thickness $e$. It is levitating above the surface due to continuous injection of vapor through the surface, with characteristic velocity $j$. The disk is inclined so that the vapor film sustaining it has a thickness $h$ on one side and $h + \Delta h$ on the other side.

*1. Lubrication equations*

Flow dynamics within the film are calculated using lubrication equations. The velocity of the vapor under the disk is denoted $u$, with symmetry imposing $\vec{u} = u\vec{e_x}$. Lubrication equation is then:

$$\frac{\partial^2 \vec{u}}{\partial z^2} = \frac{1}{\eta_v}\vec{\nabla} p(x, y) \tag{14}$$

which, by integration, gives:

$$\vec{u} = \frac{1}{2\eta_v}\vec{\nabla} p(x, y) z^2 + \vec{A} z + \vec{B}$$

The vapor velocity is null on $z = 0$, and equal to the velocity of the disk in $z = h$, so that the two boundaries conditions are $\vec{u}(z = 0) = \vec{0}$ and $\vec{u}(z = h) = \vec{V} = V\vec{e_x}$. This implies that $\vec{B} = \vec{0}$ and $\vec{A} = \frac{\vec{u}}{h} - \frac{h}{2\eta_v}\vec{\nabla} p$, so that finally:

$$\vec{u}(x, y, z) = \frac{1}{2\eta_v}\vec{\nabla} p(x, y)(z^2 - zh) + \frac{\vec{V} z}{h} \tag{15}$$

**Flow conservation.**

We denote $\bar{\vec{u}}$ the mean velocity of the vapor flow in a position (x,y) under the disk, with $\bar{\vec{u}} = \frac{1}{h(x,y)} \int_0^{h(x,y)} \vec{u}(x, y) dz$. Using equation 15, we obtain:

$$\bar{\vec{u}} = -\frac{h^2}{12\eta}\vec{\nabla} p + \frac{\vec{V}}{2} \tag{16}$$

Flow conservation then implies that $\vec{\nabla}\cdot(h\vec{u}) = j$. Using equations 13 and 16 this expression can be rewritten as:

$$\vec{\nabla}\cdot\left(h^2\vec{\nabla}p - 6\eta_v\vec{V}h\right) = -\frac{12\eta_v\lambda\Delta T}{\rho_v L_v h}. \tag{17}$$

This is made non-dimensional by introducing the following:

$$\begin{aligned}
\Pi_0 &= \frac{12\eta_v\lambda\Delta T}{\rho_v L_v R^2} \text{ and } \Pi_1 = \frac{6\eta_v V}{R}, \text{ so that} \\
\tilde{h} &= \frac{h}{R} \\
\tilde{p} &= \frac{p}{\Pi_0}
\end{aligned}$$

With the above, equation 17 can be rewritten and becomes:

$$\tilde{h}\vec{\nabla}\cdot\left(\tilde{h}\vec{\nabla}\tilde{p} - \frac{\Pi_1}{\Pi_0}\tilde{h}\vec{e_x}\right) = -1 \tag{18}$$

We solve this equation by considering small film deformations, with $\Delta h \ll h_0$, and denote $\epsilon = \frac{\Delta h}{h_0} \ll 1$, so that $h(x,y) = h_0(1 - \epsilon\frac{x}{R})$ or, in dimensionless form: $\tilde{h} = \tilde{h_0}(1 - \epsilon\tilde{x})$. Up to first order, the pressure $p$ can then be written $\tilde{p} = \tilde{p}_0 + \epsilon\tilde{p}_1 + o(\epsilon)$. We solve equation 17 at zero and first order in $\epsilon$, which gives:

$$\tilde{h_0}^4\triangle\tilde{p}_0 = -1 \tag{19}$$

$$\tilde{h_0}^4\left(\triangle\tilde{p}_1 - 3\frac{\partial\tilde{p}_0}{\partial\tilde{x}} - 4\tilde{x}\triangle\tilde{p_0}\right) + \frac{\Pi_1}{\Pi_0}\tilde{h}_0^2 = 0 \tag{20}$$

Solving (12) in cylindrical coordinates gives a solution for $\tilde{p_0}(r)$, with

$$\tilde{p_0}(r) = \frac{1-\tilde{r}^2}{4\tilde{h_0}^4} \tag{21}$$

The previous expression introduced in equation (13) gives :

$$\triangle\tilde{p}_1(\tilde{r},\theta) = -\frac{\Pi_1}{\Pi_0\tilde{h}_0^2} - \frac{11}{2\tilde{h}_0^4}\tilde{r}\cos\theta \tag{22}$$

The pressure outside the disk is constant, so that the boundary condition of equation 22 is $\tilde{p_1}(\tilde{r}=1,\theta) = 0$ , and integration finally gives:

$$\tilde{p_1}(\tilde{r},\theta) = \frac{\Pi_1}{\Pi_0\tilde{h}_0^2}\left(\frac{1-\tilde{r}^2}{4}\right) + \frac{11}{16}\frac{\tilde{r}}{\tilde{h}_0^4}(1-\tilde{r}^2)\cos\theta \tag{23}$$

*2. Forces applying on the disk*

**Normal force: pressure force** The pressure force is found by integrating the total pressure $\tilde{p}$ on the surface of the disk.

$$\tilde{F_p} = \int_S \tilde{p} dS = \int_S (\tilde{p_0} + \epsilon \tilde{p_1})\, dS \tag{24}$$

$$\tilde{F_p} = \int_S \tilde{p_0} dS + \epsilon \int_S \tilde{p_1} dS \tag{25}$$

$$\tilde{F_p} = \frac{\pi}{8\tilde{h}_0^4} \left(1 + \epsilon \frac{\Pi_1}{\Pi_0} \tilde{h}_0^2\right) \tag{26}$$

Or, in dimensional quantities:

$$F_p = \frac{3\pi}{2} \frac{\eta_v \lambda \Delta T R^4}{\rho_v L_v h_0^4} + \frac{\Delta h}{h_0} \frac{3\pi}{4} \frac{\eta V R^3}{h_0^2} \tag{27}$$

**Viscous force**. The viscous force $F_s$ is calculated by integrating the wall shear stress of the vapor flow at the bottom of the disk:

$$F_s = -\int_S \eta_v \frac{\partial u}{\partial z}_{z=h} dS, \text{ with} \frac{\partial u}{\partial z}_{z=h} \text{ derived from equation 15:} \tag{28}$$

$$\frac{\partial u}{\partial z} = (2z - h) \frac{\vec{\nabla} p}{2\eta} + \frac{V}{h} \text{ so that } \frac{\partial u}{\partial z}_{z=h} = \frac{h \vec{\nabla} p}{2\eta} + \frac{V}{h} \tag{29}$$

Once the above is integrated into expression 28, the total horizontal force can then be deduced:

$$F_s = \frac{1}{2} \int_S p \frac{\partial h}{\partial x} dS - \frac{1}{2} \int_S \frac{\partial}{\partial x}(hp) dS - \eta_v \int_S \frac{1}{1 - \epsilon \frac{x}{R}} dS \tag{30}$$

$$= -\frac{1}{2} \frac{\Delta h}{R} \int_S p dS + 0 - \frac{\eta_v V}{h_0} (\pi R^2 + 0) \tag{31}$$

$$= -\frac{1}{2} \frac{\Delta h}{R} F_p - \eta_v \frac{\pi R^2 V}{h_0} \tag{32}$$

The previous expression shows that the viscous force is the sum of two terms. The first one (arising from lubrication pressure) participates to propulsion, where the second term is a friction term, increasing linearly with the disk velocity.

*3. Horizontal and vertical balance of forces*

The total horizontal force $F_x$ that applies on the disk can now be calculated. It is equal to the sum of the pressure force (normal to the bottom of the disk) and viscous force (parallel to the disk) projected on the horizontal axis $x$. Denoting $\theta \simeq \Delta h/R$ the inclination angle of the disk, $F_x = \sin\theta F_p + \cos\theta F_s$. Since $\theta \ll 1$, $F_x$ can be simplified to:

$$F_x \simeq \theta F_p + F_s \tag{33}$$

introducing equations 27 and 32, an expression for $F$ is found:

$$F_x = \frac{\Delta h}{R} F_p - \frac{1}{2}\frac{\Delta h}{R} F_p - \eta \frac{\pi R^2 V}{h_0} + o(\frac{\Delta h}{R}) \tag{34}$$

$$F_x = \frac{3\pi}{4}\frac{\eta_v \lambda \Delta T R^3}{\rho_v L_v h_0^4}\Delta h - \eta_v \frac{\pi R^2 V}{h_0} + o(\frac{\Delta h}{R}) \tag{35}$$

The last missing parameter, $h_0$ is finally found by considering the vertical balance of forces. The disk being sustained above the surface by the pressure force, which means that its weight is compensated by the lubrication pressure generated in the film. Equalizing $F_p$ (at the first order) with the weight of the disk gives:

$$F_p = \rho_s \pi R^2 e g, \text{ from which } h_0 \text{ is deduced} \tag{36}$$

$$h_0 = \left(\frac{3}{2}\frac{\eta_v \lambda \Delta T R^2}{\rho_v L_v \rho_s g e}\right)^{1/4} \tag{37}$$

By inserting the expression for $h_0$ in the above equations, the total horizontal force that applies on the disk is fully determined. It can be written as:

$$F_x = \frac{1}{2} mg \frac{\Delta h}{R} - \eta_v \frac{\pi R^2 V}{h_0} \tag{38}$$

$F_x$ is then the sum of 2 forces, a propelling force $F_{prop} = \frac{1}{2} mg \frac{\Delta h}{R}$ and a friction force $F_f = \eta_v \frac{\pi R^2 V}{h_0}$ opposite to the propelling force. The dependency of these two forces with all dimensional parameters are the same to what is obtained through scaling laws for levitating drops (where $F_{prop} \sim \rho g R^2 \Delta h$ and $F_f \sim \eta_v \frac{R^2 V}{h}$). We expect the prefactor obtained for levitating disks to be different for gliding drops however, because of the spherical geometry.